6-4-2018

Large Rotations of Crustal Blocks in the Tjörnes Fracture Zone of Northern Iceland

Andrew J. Horst
Marshall University, horsta@marshall.edu

J. A. Carson

R. J. Varga

Recommended Citation
Horst, A. J., J. A. Karson, R. J. Varga (2018), Large rotations of crustal blocks in the Tjörnes Fracture Zone of Northern Iceland, Tectonics, doi: 10.1002/2016TC004371.

AGU100 ADVANCING EARTH AND SPACE SCIENCE

Tectonics

RESEARCH ARTICLE
10.1002/2016TC004371

Key Points:
- Mean paleomagnetic remanence directions indicate an increase in clockwise rotation of crustal blocks with proximity to the main transform fault
- Despite relatively simple curved trajectory of structures paleomagnetic, data show more complex distribution of block rotations
- Large variable rotations near transform suggest that a modified bookshelf or small block mechanism may be operating by other oceanic transforms

Supporting Information:
- Supporting Information S1
- Table S1
- Figure S1
- Figure S2

Correspondence to:
A. J. Horst,
ahorst@oberlin.edu

Citation:
Horst, A. J., Karson, J. A., & Varga, R. J. (2018). Large rotations of crustal blocks in the Tjörnes Fracture Zone of northern Iceland. *Tectonics*, *37*, 1607–1625. https://doi.org/10.1002/2016TC004371

Received 15 SEP 2016
Accepted 27 FEB 2018
Accepted article online 18 APR 2018
Published online 4 JUN 2018

Large Rotations of Crustal Blocks in the Tjörnes Fracture Zone of Northern Iceland

A. J. Horst[1], J. A. Karson[2], and R. J. Varga[3]

[1]Department of Geology, Oberlin College, Oberlin, OH, USA, [2]Department of Earth Sciences, Syracuse University, Syracuse, NY, USA, [3]Geology Department, Pomona College, Claremont, CA, USA

Abstract The interpretation of uppermost crustal deformation near oceanic transform faults is based on bathymetric lineaments and earthquake focal mechanisms, and relatively little is known about the detailed kinematics within the transform tectonized zone. The Tjörnes Fracture Zone is a broad zone of deformation produced by right-lateral transform shearing in north Iceland and is partly exposed on land providing the opportunity to study shallow-level crustal structure of mid-Miocene, thick, oceanic-like crust formed by subaerial spreading. A pronounced structural curvature of lava and dike orientations near the Húsavík-Flatey Fault within the transform zone is well documented, yet of controversial origin. In order to develop an assessment of deformation near the transform zone, samples of lavas and dikes were collected from 182 paleomagnetic sites within eight structural localities across the deformation zone on the Flateyjarskagi Peninsula. A progressive clockwise increase in locality mean remanence declinations over more than 10 km south of the fault broadly mimics the structural curvature of lava and dike orientations. Rotation estimates based on inclined rotation axes indicate significant clockwise rotation (74° ± 7° to 96° ± 9°) of multiple crustal blocks. When combined, all data from 108 sites within the deformed zone <12 km to the Húsavík-Flatey Fault yield a best fit inclined axis rotation of 55° ± 7°. The paleomagnetic data and field relationships are consistent with a modified bookshelf faulting model, with relatively small (~1 km across) independently rotated crustal blocks with variable, and in some cases large-magnitude rotations found within 10 km to the transform fault zone. Similar crustal deformation and comparable amounts of rotation may be present near other oceanic transforms, where accessibility and surficial deposits may limit documentation of more complex fault structures.

1. Introduction

Although oceanic transform faults represent geometrically simple plate boundary linkages between offset mid-ocean ridge spreading centers, few details are known of the style of deformation of the adjacent oceanic crust. Oceanic transforms exhibit a wide range of morphotectonic features, with strike-slip deformation generally accommodated within zones typically 5–10 km wide (Fox & Gallo, 1984; Kastens et al., 1986; Searle, 1986). The transform boundary zone is commonly confined to a valley with various lineaments and other features interpreted in terms of braided fault systems. However, details of how the oceanic crust accommodates transform shearing are not well resolved due to inaccessibility and abundant cover of talus, and pelagic sediment. Where exposed, transform valley walls show numerous small normal faults and only rare evidence for strike-slip motion (Francheteau et al., 1976; OTTER Team, 1985). Consequently, the general kinematics of oceanic transform faults has been inferred from abyssal hill lineament analysis and earthquake focal mechanisms.

The trends of abyssal hill lineaments on the seafloor adjacent to transforms hint at the crustal structure. For example, abyssal hill lineaments that normally form parallel to spreading centers have curved trajectories over distances of up to 20 km away as they approach transform valleys (Croon et al., 2010; Grindlay & Fox, 1993; Grindlay et al., 1991; Sonder & Pockalny, 1999). These lineaments are defined by topographic highs and intervening valleys that are the result of faulting and volcanic construction (Macdonald et al., 1996, and references therein). These structures are thought to form nearly perpendicular to the minimum compressive stress and therefore might have trends that are similar to dikes intruded below the surface. Consequently, these lineaments and dikes may be used as indicators of changes in the stress field where they initially form near transforms, or as strain markers resulting from subsequent shearing. Abyssal hill lineaments commonly deviate from ridge-parallel trends near ridge-transform intersections (Figure 1a), where they curve into the transform fault (Crane, 1976; Croon et al., 2010; Fornari et al., 1989; Fox & Gallo, 1984; Lonsdale, 1977).

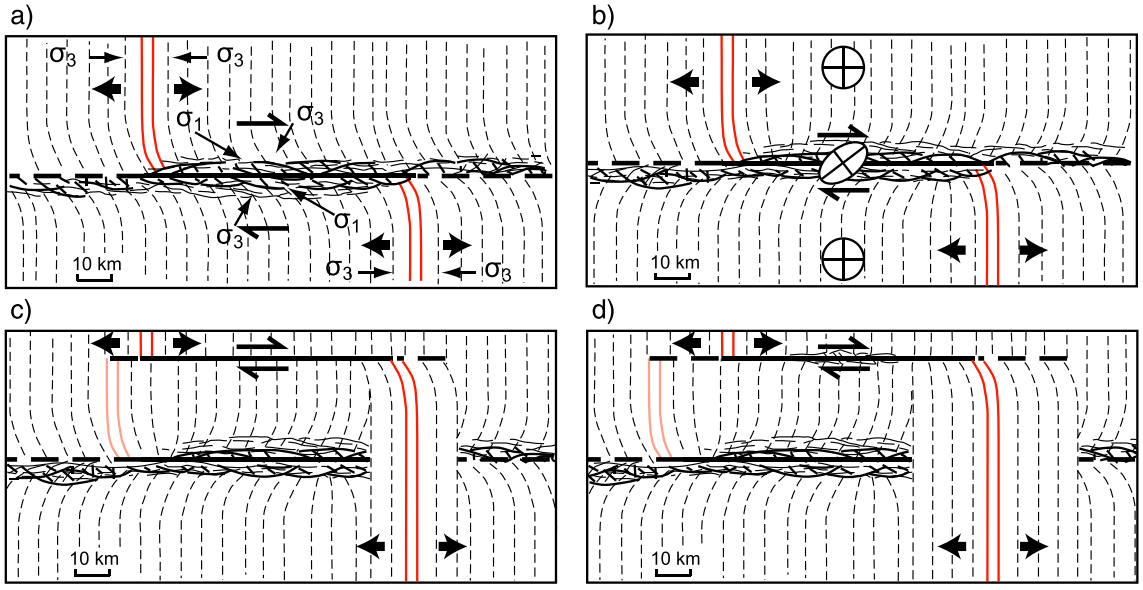

Figure 1. Schematic map-view diagrams of ridge-ridge transform faults that show different abyssal hill curvatures (after Sonder & Pockalny, 1999; Croon et al., 2010). (a) Some lineation patterns (dashed lines) are thought to be primary, stress-related features (J-shaped, or their mirror image) that form due to the stress field transition from the ridge to the transform. (b) Other curvatures are thought to be secondary, tectonically rotated features (anti-J-shaped) formed due to increased coupling across the transform. Strain ellipses show senses of shear. (c) During ridge propagation, transforms may migrate or jump with the propagating ridge tip. Inactive transform segments are truncated by new crust formed at the propagating ridge. (d) As seafloor spreading continues and slip accrues on the new transform, the crust immediately adjacent to the new transform may initially contain ridge-parallel lineaments that begin to rotate as deformation proceeds.

This so-called "J-shaped" curvature is generally explained as a result of the transition from an extensional environment along the ridge axis to the shearing regime along the transform (Fox & Gallo, 1984). These curved features persist along active portions of some transforms and are also preserved in crust beyond the active plate boundary parts of transforms along their nontransform fracture zone extensions. However, along some parts of active transform zones, lineaments curve in the opposite direction, in an "anti-J-shaped" sense (Croon et al., 2010; Sonder & Pockalny, 1999). Anti-J-shaped lineaments are interpreted as the result of tectonic rotation of lineaments by distributed deformation near the transform (Sonder & Pockalny, 1999; Tucholke & Schouten, 1988). When combined with a detailed plate motion model, these lineament patterns observed along three Pacific-Antarctic transform intersections appear to correlate with changes in the direction of plate motion (Croon et al., 2010). In all these cases, the underlying crustal structure and deformation kinematics are inferred only from the surface lineaments.

Several deformation mechanisms have been proposed to explain lineament patterns near oceanic transform fault zones as well as continental shear zones (Figure 2). Oceanic crust with mechanical anisotropy caused by ridge-parallel faults and dike margins at a high angle to the transform may represent a special case in which distributed deformation is accommodated by a series of antithetic ("bookshelf") faults (Einarsson, 1991; Tapponnier et al., 1990). In this model, crustal blocks bounded by ridge-parallel faults are rotated as deformation proceeds, and it is generally consistent with observed lineament orientations, earthquake distributions, and focal mechanisms (Cowan et al., 1986; Kleinrock & Hey, 1989; Phipps Morgan & Kleinrock, 1991; Wetzel et al., 1993). Bookshelf-type mechanisms have also been invoked to explain both structural curvature and paleomagnetic data supporting large rotations of crustal blocks near continental transform faults (Freund, 1974; Luyendyk et al., 1980; Mandl, 1987; McKenzie & Jackson, 1983; Nur et al., 1986).

The bookshelf model has also been associated with propagating rifts and microplates that result in lateral migration of the transform zones as one rift propagates at the expense of another (Hey et al., 1980; Karson, 1986; Kleinrock & Hey, 1989; McKenzie, 1986; Phipps Morgan & Kleinrock, 1991; Wetzel et al., 1993). In these cases, rift propagation requires the formation of a new transform fault in relatively older lithosphere that may be far from a preexisting transform fault. Thus, crustal deformation associated with propagating rifts and migrating transforms may occur in lithosphere with initially ridge-parallel, rather than curved, lineaments (Figures 1c and 1d). Although these propagating systems are different from typical ridge-ridge transforms,

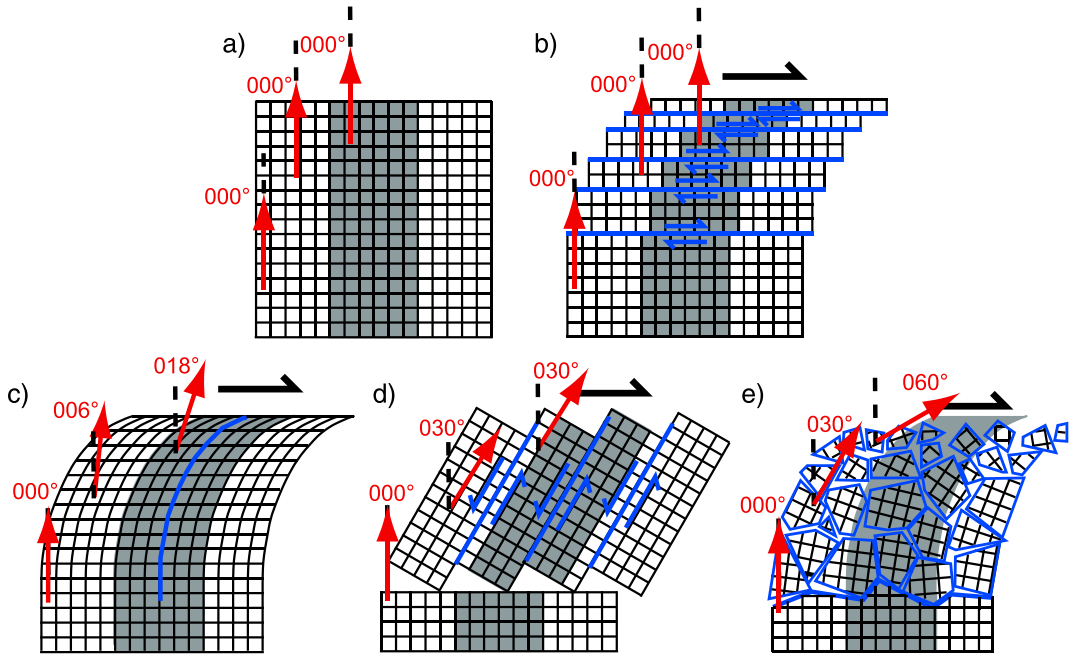

Figure 2. Models of deformation mechanisms that accommodate distributed deformation near strike-slip fault zones (after Nelson & Jones, 1987). (a) Undeformed domain with observed paleomagnetic declination (red arrow) and reference declination (black dashed line); (b) shearing on multiple faults parallel to the main shear zone with no rotation; (c) heterogeneous simple shear with a smoothly increasing strain gradient; (d) bookshelf faulting model consisting of rotated blocks bounded by faults with antithetic shear; (e) small block model with variable rotation.

the distributed deformation associated with curved (anti-J-shaped) lineaments observed near some oceanic transforms may also be accommodated by a bookshelf faulting mechanism. However, the kinematic details of upper crustal deformation in these zones are difficult to assess from lineament analysis and earthquake focal mechanisms alone.

In northern Iceland, the Tjörnes Fracture Zone links subaerial spreading in the Northern Volcanic Zone to the offshore Kolbeinsey Ridge through a wide zone of distributed deformation related to the right-lateral transform system. A main transform fault strand is located offshore near the northern coastline of the Flateyjarskagi Peninsula, providing an opportunity to study the structure and kinematics of uppermost oceanic-crust immediately adjacent to a major transform fault. In this paper, we present paleomagnetic data from basaltic lavas and dikes from numerous sites across the Flateyjarskagi Peninsula to investigate the origin of structural curvature and assess proposed deformation mechanisms. Paleomagnetic sites are located in four main study localities (coherent blocks) with increasing distance away from the major offshore Húsavík-Flatey Fault (HFF) Zone, and four subsidiary study localities adjacent to the fault zone to assess directional consistency and distinguish between different deformational models. These data may be relevant to the interpretation of deformation adjacent to major oceanic transforms and have implications on the tectonic evolution of northern Iceland, (Bergerat, Angelier, & Homberg, 2000; Bergerat, Angelier, & Villemin, 1990; Garcia et al., 2002; Homberg et al., 2010; Sæmundsson, 1974; Young et al., 1985). Collectively, the results and available structural data show that deformation in northern Iceland is considerably more complex than can be accounted for by typical deformation models from strike-slip fault zones. These data also offer a unique analog for details of deformation accommodated within migrating transform fault zones associated with propagating rifts and microplates.

2. Tectonic Setting

2.1. Subaerial Spreading Systems in Iceland

The tectonic evolution of the plate boundary zone across Iceland has largely been controlled by the interaction between rifting of the subaerial Mid-Atlantic Ridge system and the pronounced effect of the Iceland hot spot or mantle plume (Einarsson, 2008; Sæmundsson, 1979). This interaction has resulted in an unstable plate

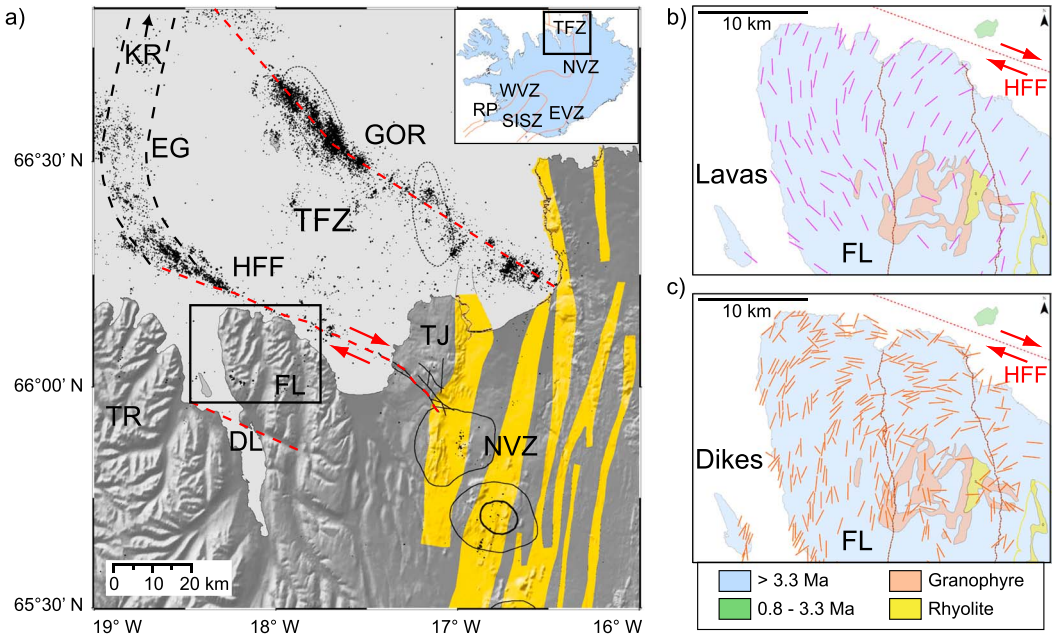

Figure 3. Structures and seismic activity in Tjörnes Fracture Zone and Flateyjarskagi Penninsula in North Iceland. (a) Seismicity occurs primarily within two NW-SE trending zones north of Iceland within the broad region of deformation called the Tjörnes Fracture Zone (TFZ). The red dashed lines show trends of three main structural features: Grímsey Oblique Rift (GOR), Húsavík-Flatey Fault (HFF), and Dalvík Lineament (DL). The black dashed line is Eyjafjarðaráll Graben (EB), the southern extension of the Kolbeinsey Ridge (KR). The yellow swaths show locations of active volcanic systems within the Northern Volcanic Zone (NVZ). Peninsula labels are Flateyjarskagi (FL), Tjörnes (TJ), and Tröllaskagi (TR). The small inset map shows location of TFZ in North Iceland and locations of other active plate boundary zones: Reykjanes Peninsula (RP), Western Volcanic Zone (WVZ), South Iceland Seismic Zone (SISZ), Eastern Volcanic Zone (EVZ), and Northern Volcanic Zone (NVZ). Maps (b) and (c) show the clockwise curvature with proximity to the HFF of strikes of lava flows (thin purple lines) and steeply dipping dikes (orange lines), respectively (after Young et al., 1985).

boundary system that has caused the Icelandic rift zone to relocate at least two or three times throughout the last 15 Ma (Hardarson et al., 1997). Through time, the rift zone tends to migrate northwestward with respect to the underlying hot spot, resulting in progressive southeastward relocation of the spreading axes in order for the active rift zone to remain above the hot spot magmatic source (Hardarson et al., 1997; Pálmason & Sæmundsson, 1974; Sæmundsson, 1974, 1979). Although the mechanism of rift relocation is debated, it is generally considered to take place by discrete rift jumps on land (Hardarson et al., 1997), whereas evidence for propagation exists both onshore in south Iceland (LaFemina et al., 2005) and offshore south of Iceland along the Reykjanes Ridge (Benediktsdóttir et al., 2012; Hey et al., 2010).

The most recent eastward shift of the active rift zone in Iceland has offset the plate boundary and resulted in the formation of two transform boundary zones, the South Iceland Seismic Zone and the Tjörnes Fracture Zone, respectively. The South Iceland Seismic Zone accommodates left-lateral shearing between the Western and Eastern Volcanic Zones in a narrow (20 km N-S) by ~60-km-wide E-W-trending zone and is marked by distinct N-S trending arrays of en echelon surface fractures, the surface expressions of underlying seismogenic strike-slip faults. The N-S-striking faults accommodate overall left-lateral shearing by right-lateral slip on faults that rotate counterclockwise as deformation proceeds, thus defining a bookshelf faulting model for south Iceland (Einarsson, 1991; Einarsson & Eiríksson, 1982; Sigmundsson et al., 1995).

2.2. Tjörnes Fracture Zone

The Tjörnes Fracture Zone (TFZ) is a broad region of deformation in northern Iceland thought to have formed ~7 Ma to accommodate right-lateral transform shearing between the Northern Volcanic Zone and the Kolbeinsey Ridge offshore (Sæmundsson, 1974; Ward, 1971). Most of the transform boundary zone occurs offshore over a large area, approximately 150 km (E-W) by 75 km (N-S), and consists of major NW-SE striking fault zones and left-stepping, en echelon, N-S trending bathymetric troughs (or grabens) and volcanic fissure swarms (Magnúsdóttir et al., 2015; McMaster et al., 1977). Based on the distribution of seismic activity (Figure 3a), most of the deformation is accommodated along two main NW-trending zones, the HFF Zone

and the Grímsey Oblique Rift zone (Einarsson, 1991, 2008). The Grímsey Oblique Rift appears to consist of four left-stepping, en echelon, N-S trending volcanic systems, similar to those in the Northern Volcanic Zone (Brandsdóttir et al., 2003). The HFF Zone was thought to be the main structure of the Tjörnes Fracture Zone (Rögnvaldsson et al., 1998), and it can be traced continuously over 75 km WNW from the Northern Volcanic Zone to the Eyjafjarðaráll Graben, the southern amagmatic extension of Kolbeinsey Ridge. Einarsson (1976) showed that other zones might be just as important in accommodating the transform motion, and Metzger and Jónsson (2014) confirmed by GPS measurements that about two thirds of the plate motion is taken up by the Grímsey Oblique Rift. A third and southernmost NW trending seismic zone, the Dalvík Lineament (Einarsson, 1991), has been suggested to represent a weak southern margin of the Tjörnes Fracture Zone where the southern tips of N-S striking faults terminate (Stefansson et al., 2008). Focal mechanisms of most large earthquakes in the Tjörnes Facture Zone indicate a NW-SE striking and a NE-SW striking fault planes (Einarsson, 1987), consistent with dextral slip on major NW striking faults or sinistral slip on NNE striking faults expected for a bookshelf faulting mechanism. Neither the HFF Zone nor the Grímsey Oblique Rift are orthogonal to Kolbeinsey Ridge or the Northern Volcanic Zone, and based on the current plate motion direction (~106°; DeMets et al., 2010), the Tjörnes Fracture Zone is slightly transtensional.

The HFF Zone is partly exposed on land on the peninsulas of Flateyjarskagi and Tjörnes, and numerous studies document the structure of the uppermost crust (e.g., Fjäder et al., 1994; Jancin et al., 1985; Långbacka & Gudmundsson, 1995; Sæmundsson, 1974; Young et al., 1985). Available K/Ar whole-rock data indicate Miocene-age basalts ranging from 11.9 ± 1.2 to 8.9 ± 0.8 Ma across northern Flateyjarskagi. These older lavas are unconformably overlain by lavas younger than 6.3 ± 0.2 Ma in the eastern portion of the peninsula (Jancin et al., 1985). The older sequence of basalt lavas have gentle (≤12°) S/SW dips in southern Flateyjarskagi becoming progressively steeper to the north with dips greater than 40° to NW near the north coast (Young et al., 1985). Near the middle of the peninsula, nearly horizontal lavas can be traced to the east where they then increase in dip to more than 30° SE within the Dalsmynni flexure zone below the unconformity (Young et al., 1985). The overall structural geometry of the Miocene-age lavas on Flateyjarskagi approximates a S/SW trending and shallowly plunging antiform. Younger, mostly Pliocene-age lavas above the unconformity have gentle dips typically less than 10° ESE (Young et al., 1985).

One of the major structural patterns revealed from detailed field mapping and measurements is a pronounced curvature of both lava flow and dike strikes across Flateyjarskagi (Figures 3b and 3c). From south to north, a progressive clockwise-curvature of lava flow strikes with increasing dip magnitudes is observed over a wide area approaching the HFF Zone (Young et al., 1985). A similar progressive clockwise-curvature of dike strikes occurs across the peninsula from approximately NNE (010°) to nearly parallel to the HFF (~110°; Young et al., 1985).

The origin and interpretation of this structural curvature is the subject of debate (Gudmundsson & Fjäder, 1995; Jancin et al., 1995). In one view, the progressive clockwise change in dike and lava orientations (strike) was interpreted to signify heterogeneous shear strain to accommodate transform deformation and structural rotations of up to 90 to 110° within a zone extending ~11 km south of the HFF (Young et al., 1985). Alternatively, the structural curvature has also been interpreted as the result of the orientation of the stress field during their intrusion, and thus a primary feature where no tectonic rotations have occurred except in the narrow zone (~2 km) adjacent to the HFF (Fjäder et al., 1994). These competing interpretations yield the opposite sense of shearing across the transform.

Brittle deformation features are common throughout Flateyjarskagi (Figure 4), with an increase in density of faults and fractures with proximity to the northernmost outcrops where the HFF is partly exposed with locally intense faulting, fracturing, and veins (Bergerat et al., 2000; Fjäder et al., 1994; Young et al., 1985). The major 3- to 5-km-wide damage zone consists of large-scale faults exhibiting breccia, cataclasite, and gouge zones parallel to the trend of the HFF (~295°). In addition to these subvertical WNW striking dextral strike-slip faults, another common set of faults appear to be steeply dipping NNE striking sinistral-normal oblique-slip faults. These arrays of faults bound small coherent blocks of fractured lavas and dikes a few tens to hundreds of meters across and are also cut by numerous small-scale faults and veins in various orientations.

Farther south away from the HFF zone, the deformation is much less intense and more focused into discrete fault zones that generally change strikes from NE-SW in the north to NNE-SSW to N-S in the southern part of

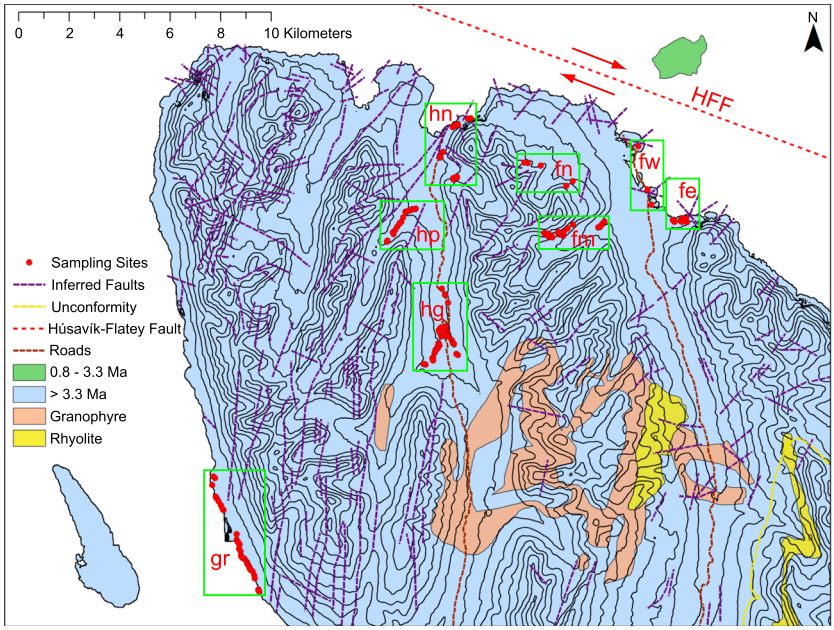

Figure 4. Geologic context of paleomagnetic sites within focused study localities (green boxes) on Flateyjarskagi. Most sites are located within main study localities (fm, hp, hg, and gr) with fewer sites in subsidiary localities (fe, fw, fn, and hn) nearest to the HFF. Faults after Young et al. (1985).

the peninsula. Farther south from the north coast, some sections of lava are very coherent over distances of several hundred meters to a few kilometers as they exhibit similar orientations and no evidence of significant internal deformation. The southern boundary of the main HFF zone is not clear, although it has been proposed to coincide with the Gil-Látur Line, ~11 km south of the HFF (Young et al., 1985).

Although many faults occur throughout the peninsula, the lack of offset markers makes the displacement magnitudes difficult or impossible to determine. Damage zones and fault cores are typically less than 1 m wide, suggesting that displacements are relatively small (few to tens of meters). However, maximum throws on faults near the northern coastline may be as much as 1,000 m (Young et al., 1985). Overall, estimates of total displacement on HFF range from 20 (Young et al., 1985) to 60 km (Sæmundsson, 1974).

3. Field and Laboratory Methods

Paleomagnetic remanence data were collected for 1,292 oriented core samples from 182 sites distributed across the Flateyjarskagi Peninsula in northern Iceland. Most (142) sites are located within one of four main study localities, Grenivík (gr), Gil (hg), Pverá (hp), and Mosahnjúkur (fm) each at decreasing distance to the HFF Zone, while the remaining 40 sites are located within four subsidiary localities more proximal and parallel to the fault zone (Figure 4 and Table S1). At each field site, typically eight standard 2.5-cm diameter core samples were drilled from either a basalt lava or dike using a gasoline-powered drill. All samples were oriented with magnetic compass, and also oriented with a Sun compass when conditions were favorable. Comparison of the two orientation methods indicates no significant bias in azimuths determined with magnetic compass, and corrections to specimen azimuths based on Sun compass readings are consistent with a magnetic declination nearly identical to the International Geomagnetic Reference Field declination at the site (approximately −16°). Lava orientations were determined from multiple measurements on the contacts between flows at each sampling site and supplemented with data from published maps (e.g., Young et al., 1985).

Paleomagnetic remanence measurements and demagnetization were conducted on a 2G Enterprises cryogenic magnetometer in a shielded room at Scripps Institution of Oceanography. Specimens from each site were progressively demagnetized using thermal or alternating field (AF) techniques through a complete spectrum of demagnetization levels. For AF demagnetization experiments, specimen remanent magnetization was measured following applied field magnitudes of 5, 10, 15, 20, 25, 30, 40, 50, 60, 70, 80, 90, 100,

120, 150, and 180 mT. Thermal demagnetization was performed in 14 (or 19) steps: 100, 150, 200, 250, 300, 350, 400, 450, 475, 500, 520, 540, 560, and 580°C (600, 620, 640, 660, and 680°C). Magnetization components were determined by principal component analysis (Kirschvink, 1980) using at least four or more steps with maximum angular deviation <5°. Mean directions for each site were calculated from characteristic remanent magnetization (ChRM) directions of specimens based on Fisher statistics (Fisher, 1953). Bootstrapped site mean vectors were used to calculate mean directions and uncertainties at the study locality level (Tauxe et al., 1991), and structural tilt corrections about present strike directions were applied based on average lava orientations measured in each study area. In one study area (fw) where only dikes were sampled, average lava orientations were determined from field measurements on adjacent lavas combined with data from published maps (e.g., Young et al., 1985). Additional bootstrap tests for common mean directions (Tauxe, 2010) was implemented for reversals tests, and for determining statistical distinction of mean lava to dike directions, different locality mean directions, and locality mean directions to expected reference directions. Measured directions were compared to an expected time-averaged direction produced by a geocentric axial dipole (GAD) field in north Iceland (dec = 000°/inc = 77.5°). Paleomagnetic analyses of lavas (<15 Ma) in Iceland broadly support the GAD hypothesis that maintaining the present dipole direction is a valid reference direction (e.g., Kristjánsson, 2009; McDougall et al., 1984). European and North American reference Apparent Polar Wander Paths indicate essentially indistinguishable expected directions for north Iceland during the last 15 Ma, with uncertainty on poles less than 5° (Besse & Courtillot, 2002).

4. Results

4.1. Paleomagnetic Remanence

The arithmetic mean natural remanent magnetization intensities of lavas and dikes measured in this study is 5.1 Am^{-1} (geometric mean = 2.7 Am^{-1}), with dike natural remanent magnetization values (6.2 Am^{-1}) slightly higher than lavas (4.1 Am^{-1}). Most of remanence data from lava and dike specimens reveal high-stability, dominantly single-component remanences (ChRM) with average maximum angular deviation <2.2°, after removal of minor overprints typically by 15 mT or 200°C (Figure 5). Unblocking occurs over a wide range of temperatures with maximum unblocking temperatures invariably between 500 to 580°C, suggesting remanence carried by low-Ti titanomagnetite. Few specimens exhibit a higher unblocking temperature (580C to 680°C) hematite component typically nearly parallel to the highest unblocking temperature magnetite component. The median destructive field, or the AF that reduces the vector difference sum of remanence to half its initial value, was calculated as a metric for specimen stability. In an analogous manner, the median destructive temperature was calculated for thermally demagnetized specimens. Lavas and dikes typically have moderate stability with a mean median destructive field of 29 mT and mean median destructive temperature of 357°C.

Although most specimens are well behaved and reveal simple, linear components, a few dike and lava specimens show more complex multiple component remanences. These few specimens are excluded from the Fisher mean calculation at the site due to partial to nearly complete overlap between unblocking temperature spectra that precludes isolation of a stable component using a linear-fit. In some sites from dikes, multiple specimens show antipodal components over a range of different partially overlapping laboratory unblocking temperature spectra (Figure 5g). In these cases, the highest laboratory unblocking temperature component is regarded as the stable ChRM. Only a few specimens are excluded from the Fisher mean calculated for each site due to one of the following behaviors: directions from AF demagnetization that significantly differ from those isolated by thermal demagnetization and overlapping coercivity or laboratory unblocking spectra that precluded isolation of a linear ChRM.

Estimated site mean directions with ≥4 specimen ChRM directions and 95% confidence limits (α_{95}) ≤ 15° are considered reliable, though most of site means are based on at least 5 specimens and are well determined with $\alpha_{95} < 10°$ (>50% sites have $\alpha_{95} < 5°$; Figures 6 and 7 and Table S1). However, data from 19 sites are rejected from further analysis due to either the inability to determine a reliable or significant site mean direction, or a highly discordant site mean direction compared to other sites within the same area. Of the total rejected, nine site mean directions are rejected due to either multiple unstably magnetized specimens within the site, or all specimens were stable but considerably dispersed in direction with very large 95% confidence limits. The additional 10 site mean directions that are removed from the analysis exhibit highly discordant

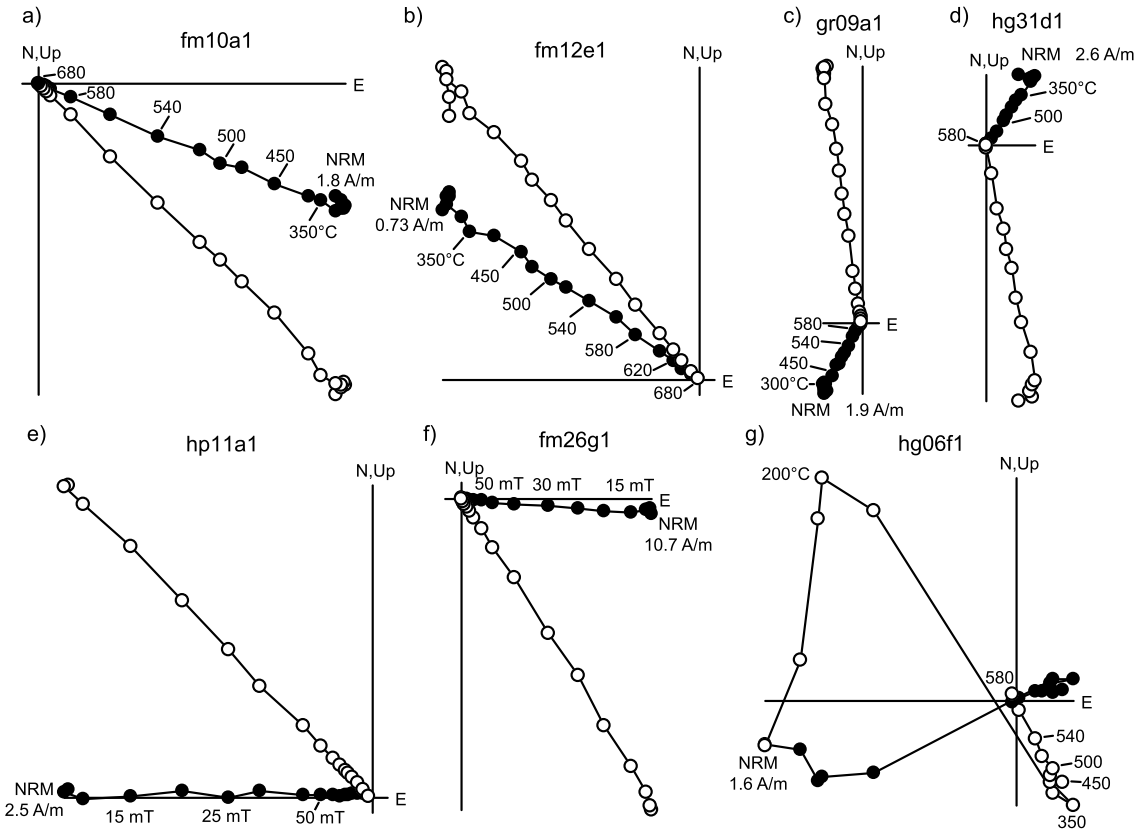

Figure 5. Typical alternating field and thermal demagnetization behavior, indicating the dominance of single components of magnetization following the removal of minor overprints. The solid (open) circles are the horizontal (vertical) projections. Diagrams a, b, c, and e are from lava specimens, while d, f, and g are from dikes. (g) Example of one of the few multicomponent magnetizations from a dike revealed during stepwise thermal demagnetization.

directions (>45°) away from either positive or negative inclination groups of the area (average angular difference ~87°).

Site mean directions with positive or negative inclinations pass a bootstrap reversal test in only the southernmost main study locality (gr) indicating that the antipodal directions are consistent with normal and reverse polarities, respectively. In all seven other localities closer to the fault zone, directions tend to exhibit streaked distributions, and thus, directional groups with positive and negative inclinations do not pass the reversal test at the 95% confidence level. However, the directions in these areas are nearly antipodal, and thus, directions with negative inclinations interpreted as reverse polarity are flipped to their antipodes, and a bootstrap of site mean directions yields locality mean directions in each study locality (Table 1). Within each of the focused study localities, bootstrapped site mean directions are well determined with relatively low major (η_{95}) and minor (ζ_{95}) semiangles of 95% confidence (Figures 6 and 7 and Table 1).

Within some study localities, site mean directions show variably streaked distributions. When site mean directions from dikes and lavas within a locality are plotted separately, it appears that a few localities show statistically distinct in situ lava and dike directions with consistently more clockwise and shallow lava directions than dikes (Figure 8). Although the subsidiary localities do not show distinct directions based on formation type or dike orientation, they do show a similar tendency for more clockwise and shallow directions from lavas flows. Upon closer inspection of the streaked directions from lavas in the hg area, it appears that there are two distinct paleomagnetic directions from lavas closer and farther from the fault zone (i.e., northern and southern parts of area hg). Furthermore, the mean direction from the northern group lavas is distinct from the mean dike direction, whereas the southern lavas and dikes have indistinguishable directions. The abrupt change in remanence directions from north to south parts in locality hg occurs at a distance of ~12 km south from the HFF and also coincides with distinct changes in lava and

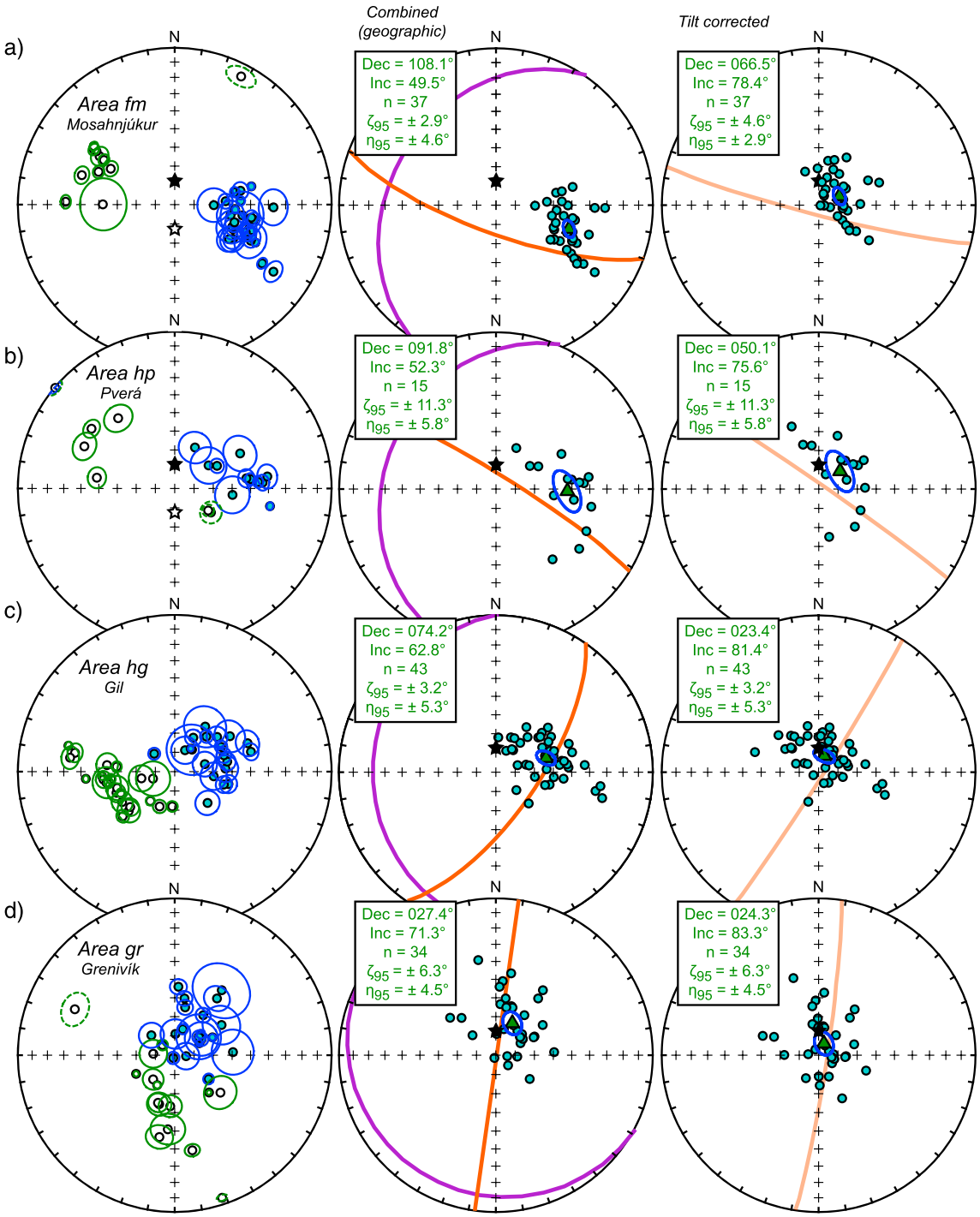

Figure 6. Equal-area, lower-hemisphere projection stereonets of paleomagnetic remanence directions for all reliable sites in each of the four main study localities across Flateyjarskagi (see Figure 4 for locations). Site mean directions and corresponding α_{95} confidence ellipses are shown (left). The few directions with dashed ellipses represent sites with discordant directions not included in locality mean calculation. Locality mean directions (center) determined from bootstrap of site mean directions after flipping reverse directions to antipodes, and tilt-corrected mean directions for each of the four main study localities are also shown (right). The filled (open) circles plotted in lower (upper) hemisphere. The filled (open) star represents geocentric axial dipole expected direction at ~66°N for normal (reverse) polarity. The great circles indicate average lava flow (purple) and dike (orange) orientations before (center) and after tilt correction (right). Bootstrapped locality mean directions from the three northernmost areas are distinct from the expected direction at the 95% level of confidence, suggesting that some relative rotations have occurred.

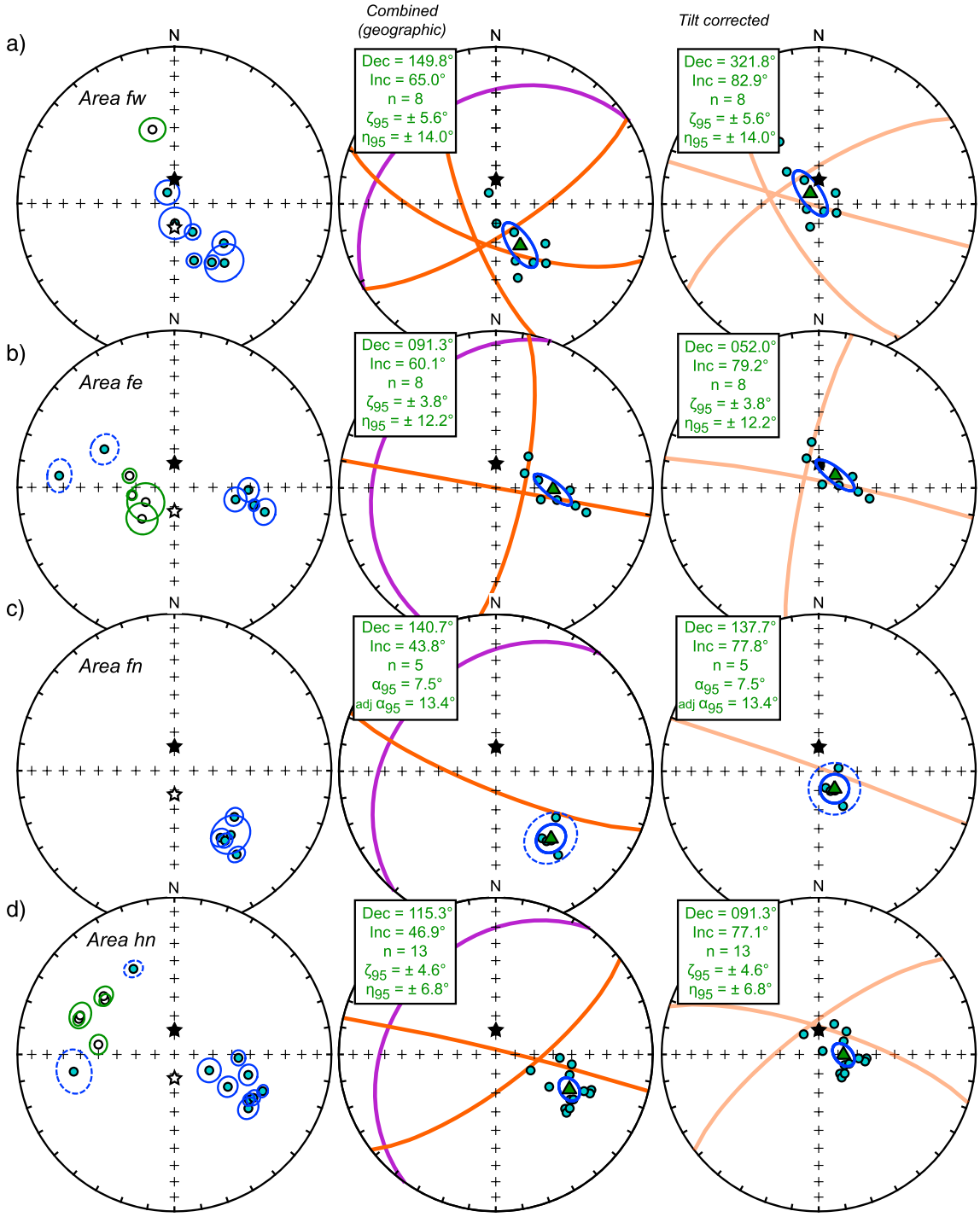

Figure 7. Equal-area, lower-hemisphere projection stereonets of paleomagnetic remanence directions for sites in each of the subsidiary study localities along the northern part of Flateyjarskagi (see Figure 4 for locations). Same symbols and layout as shown in Figure 7. The dashed ellipse around locality fn mean shows increased uncertainty due to low number of sites (see discussion).

dike orientations (Figure 8). The abrupt changes in orientations occur subtly over a few hundred meters distance and in the general location of the Gil-Látur Line proposed by Young et al. (1985) as a structural boundary across which the deformation increases more dramatically toward the north. As a result, the hg locality is treated as two separate localities (hg-n and hg-s).

Table 1
Locality Mean Paleomagnetic Results

		In situ							Average lava		Tilt corrected		Best fit			
		Directions							Orientation		Directions		Inclined axis			
Loc[a]	Dist[b]	Dec[c]	Inc	N/N$_t$[d]	η_{95}[e]	ζ_{95}	α_{95}[f]	CSD	Strike[g]	Dip	DD	Dec[h]	Inc	R ΔR[i]	Axis[j]	Angle
fw	3.0	149.8	65.0	8/9	14.0	5.6	12.6	18.0	238	32	NW	321.8	82.9	38 ± 29	172/83	−145 ± 29
hn	4.3	115.3	46.9	13/16	6.8	4.6	6.4	12.4	216	32	NW	91.3	77.1	−91 ± 9	170/68	−96 ± 9
fe	4.3	91.3	60.1	8/10	12.2	3.8	10.7	15.4	185	26	NW	52.0	79.2	−52 ± 21	178/66	−56 ± 21
fn	4.4	140.7	43.8	5/5	-	-	(13.4)[l]	7.9	232	34	NW	137.7	77.8	−138 ± 16	170/69	−93 ± 16
fm	6.4	108.1	49.5	37/39	4.6	2.9	4.0	13.5	212	33	NW	66.5	78.4	−67 ± 7	181/62	−74 ± 7
hp	8.2	91.8	52.3	15/18	5.8	11.3	9.8	20.1	203	29	NW	50.1	75.6	−50 ± 16	175/58	−57 ± 16
hg-n	11.4	86.2	55.8	22/23	6.2	4.5	5.7	14.8	190	26	NW	60.1	80.5	−60 ± 10	159/68	−66 ± 10
hg-s	12.5	55.5	68.3	21/22	5.8	13.7	5.0	12.7	173	20	SW	349.6	80.1	10 ± 13	173/00	−23 ± 13
hg	12.1	74.2	62.8	43/45	5.3	3.2	4.5	16.5	182	23	NW	23.4	81.4	−23 ± 11	180/45	−31 ± 11
gr	22.5	27.4	71.3	34/40	4.5	6.3	5.7	18.2	119	12	SW	24.3	83.3	−24 ± 6	119/00	−12 ± 6
All N[k] sites	< 12	105.4	53.7	108/120	2.6	3.6	3.2	18.5	225	32	NW	65.2	80.3	−65 ± 7	194/52	−55 ± 7

[a]Locality: abbreviated study locality names. [b]Dist: Average site distance (km) south from Húsavík-Flatey Fault. [c]Dec and Inc: Declination (°) and inclination (°) of bootstrapped site mean directions in geographic coordinates. [d]N/N$_t$: Number of sites included in mean/total number of sites in study locality. [e]η_{95}, ζ_{95}: Semiangle of major, minor axis of ellipse of 95% confidence. [f]α_{95}, CSD: Fisher circle of 95% confidence (°), and circular standard deviation. [g]Strike, dip, and dip direction (DD): Average orientation of lavas based on field measurements and published maps (e.g., Young et al., 1985) [h]Dec and Inc: Declination (°) and inclination (°) of bootstrapped site mean directions in tilt-corrected coordinates. [i]R ΔR: Residual vertical-axis rotation after tilt-correction, with ΔR uncertainty (after Demarest, 1983); positive rotation value is clockwise restoration and negative rotation is counterclockwise restoration. [j]Axis, Angle: Best fit axis and angle (°) of net tectonic rotation with ΔR uncertainty (after Demarest, 1983). [k]All northern sites; tilt-corrected direction based on combined mean after individual tilt correction for each locality, see main text for discussion, and Figure S2. [l]Only adjusted α95 value for locality fn is shown, instead of calculated value of 7.5°, see main text for discussion, and Figure S1.

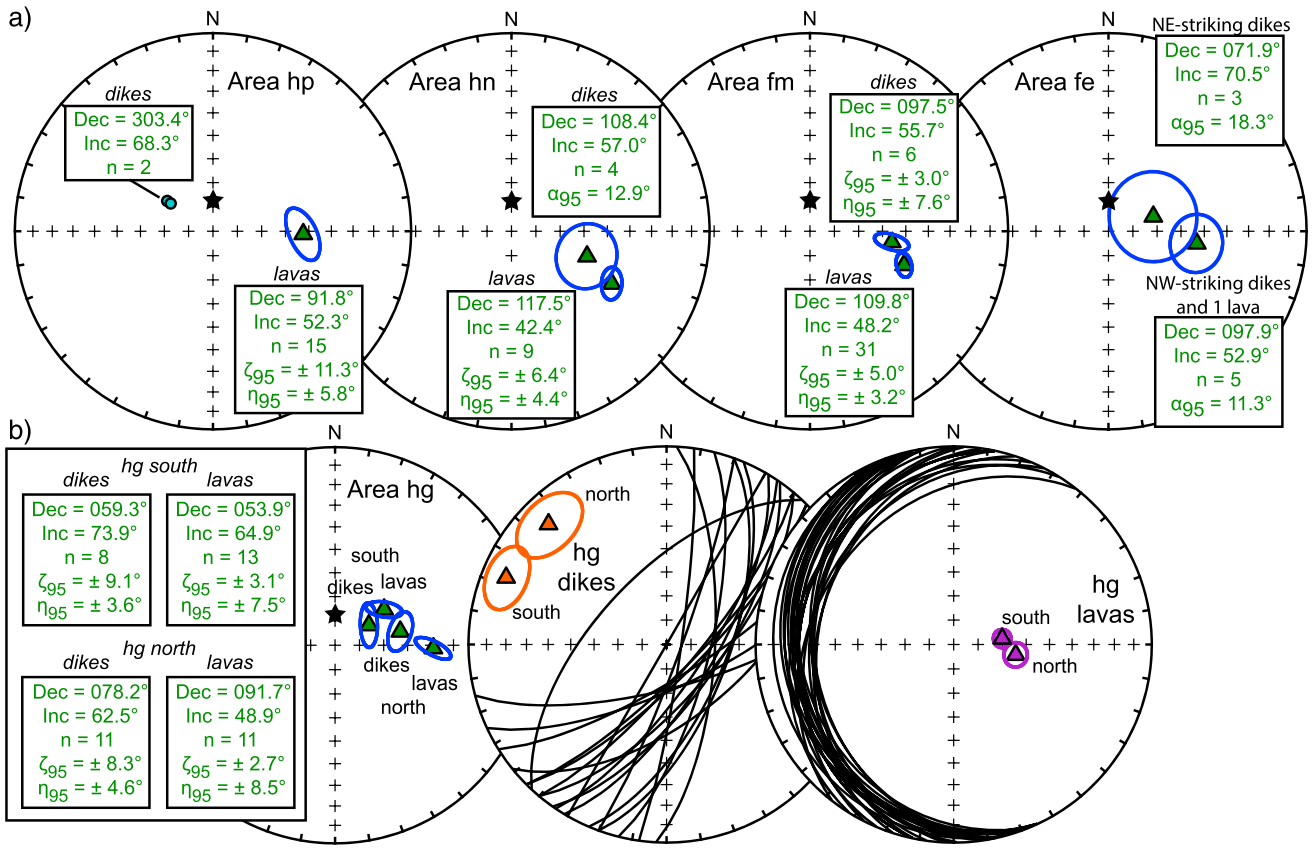

Figure 8. Equal-area, lower-hemisphere projection stereonets show details of paleomagnetic and structural data. (a) Mean dike and lava remanence directions within localities hp, hn, and fm, and mean directions from different dike orientations in locality fe. All reverse polarity directions shown in normal polarity for comparison. Note consistently clockwise and shallower lava directions than dikes in each locality. (b) Locality hg also shows statistically distinct mean lava and dike remanence directions, and orientations of mean dike poles and lava poles from northern and southern portions of the locality.

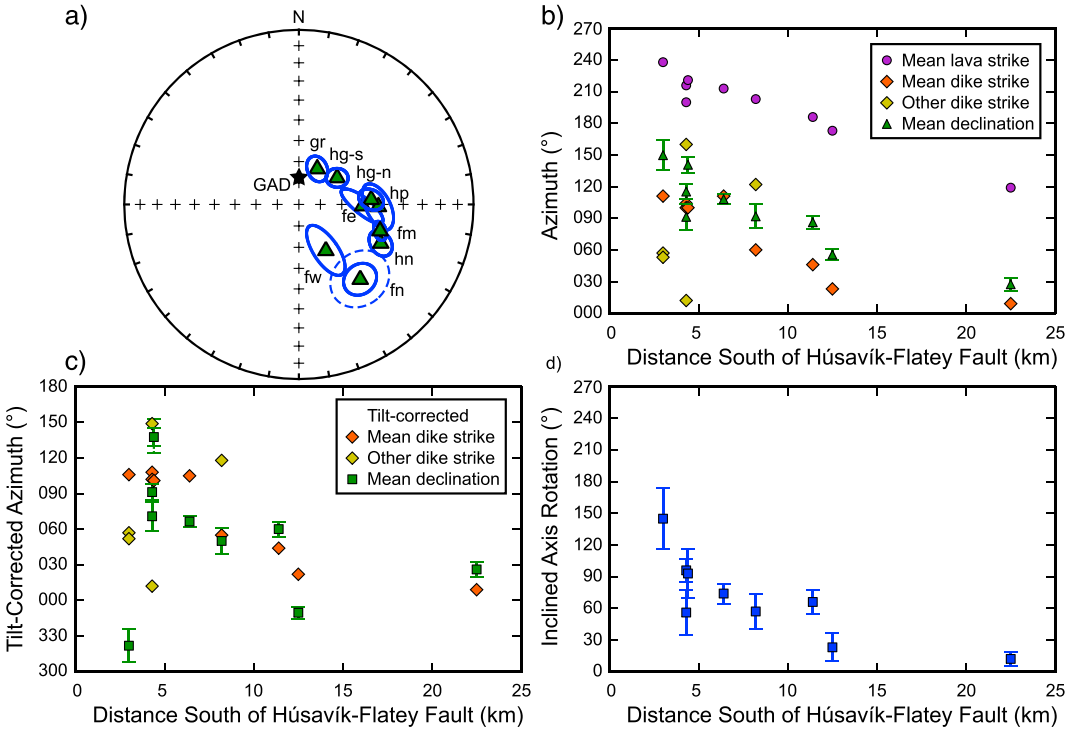

Figure 9. (a) Equal-area, lower-hemisphere projection stereonet of the locality mean paleomagnetic remanence directions for all reliable sites in each study locality shown with corresponding bootstrapped confidence ellipses in geographic coordinates. The filled circles plotted in lower hemisphere, and the filled star represents geocentric axial dipole (GAD) expected direction. The dashed α_{95} ellipse around fn direction represents increased uncertainty due to small number of sites. Scatter plots illustrate azimuthal variation in locality mean remanence declinations, mean lava strike, mean dike strike, and other (less common) dike strikes for each locality with proximity to HFF in (b) geographic coordinates and (c) after tilt-correction. (d) Also shown is the variation in amounts of rotation about the best fit inclined axis for each study locality as a function of distance from the HFF.

4.2. Comparing Locality Mean Directions

All locality mean directions are statistically distinguishable from the GAD expected direction, and many are also clearly distinct from one another (Figure 9a). However, distinguishing directions among a few adjacent study localities is more challenging due to overlapping 95% confidence limits that do not include the mean, and relatively few sites in subsidiary localities most proximal to the HFF. When only confidence limits of (bootstrapped) mean directions overlap but do not include the mean direction, additional statistical tests are required to determine whether two estimated remanence directions are distinct. A bootstrap test for common mean directions (Tauxe, 2010) between the study localities with partially overlapping uncertainties (fm, hp, and hg-n, and fe) reveals that directions from area fm are distinguishable from hg-n and fe; however, directions from hp are indistinguishable from hg-n and fe localities.

5. Discussion

The observed patterns in integrated paleomagnetic remanence directions and structural data within the study localities and among different localities have significant implications for the interpretation of deformation adjacent to the HFF and other oceanic transform systems. However, accurate interpretations of the magnitude of crustal block rotations and other deformation features rely heavily on the combination of these paleomagnetic data with structural field relationships, as well as any assumptions. The reliability of paleomagnetic and structural data to determine tectonic rotations depends on at least three key assumptions: (1) the locality mean remanence was acquired over a sufficient amount of time to average secular variation of the geomagnetic field, and the initial (predeformation) mean directions coincide with the time-averaged GAD field; (2) the observed stable remanence directions predate both vertical axis structural rotations and horizontal axis tilting; and (3) little internal deformation of each lava flow and dike results in a constant angle between the remanence vector and the normal to the igneous unit during deformation. Assumptions (2) and

(3) appear valid and justified due to the presence of nearly antipodal directions in many study areas, and lack of pervasive brittle structures within sampled units in all but the locality closest to the HFF zone (fw). However, due to the low number of sites in a few localities, it is necessary to first investigate whether remanence vectors within these few areas exhibit appropriate scatter anticipated due to secular variation. After examination of the validity of assumption (1), we then highlight key trends in the paleomagnetic and structural data, explore different approaches to estimating rotation, assess the most plausible deformation mechanisms to accommodate the rotations, and finally discuss potential implications for other oceanic transforms.

5.1. Investigation of Sufficient Averaging of Secular Variation

Due to the large scatter in directions expected at high latitudes, caution must be exerted when interpreting directions from localities with only 5 to 10 sites. To assess whether the estimates of uncertainty from the few sites within localities proximal to the fault have underestimated uncertainty produced by secular variation, we develop a bootstrap analysis of a previous data set of lavas from the Northwest Fjörds in Iceland (Kristjánsson, 2009). The data were filtered to remove site mean vectors with $\alpha_{95} > 10°$, or virtual geomagnetic poles $<45°$ (Figure S1a), with the later being a procedure commonly implemented in paleomagnetic studies that are not concerned with transitional fields. We resample the remaining 333 directions 1,000 times at random, each psuedosample with $N = 5$, and then calculate Fisher parameters of each of these sets of pseudodata to investigate the dependence of α_{95} and CSD on number of sites (N) per area. Repeating this exercise for variable numbers of N (e.g., multiples of 5) demonstrates that the uncertainty calculated for area fn ($N = 5$) is likely underestimated (Figure S1b). Based on this analysis, we choose to increase the α_{95} uncertainty to the average α_{95} of 13.4° (for $N = 5$) to mimic that demonstrated from this exercise, rather than group area fn sites with an adjacent area to increase N. We note that the other two areas (fw and fe) that have $N = 8$ show uncertainties that are consistent with the range determined in this exercise, and uncertainties from all other areas are also within the range for comparable N (Figure S1b).

5.2. Interpretation of Trends in Paleomagnetic and Structural Data

Patterns in paleomagnetic remanence directions and structural data within the study localities and differences among the localities have significant implications for the interpretation of deformation adjacent to the HFF. A few specific trends include the streaked distribution of remanence directions, statistically distinct lava and dike remanence directions in a few study localities, and distinguishable directions from localities both perpendicular and parallel to the HFF.

Within a few study localities, site mean remanence directions show streaked distributions that may be produced by synkinematic emplacement of lavas or dikes during tectonic rotation and may also explain why data from most localities do not pass a reversals test. The abrupt change in remanence directions across locality hg, and the accompanying subtle change in orientations of lavas and dikes, is consistent with the location of the Gil-Látur Line and confirms that this is a unique structural boundary across which some rotation of different crustal blocks has occurred. However, the distinctly more clockwise and shallow lava directions than those from dikes in hg-n and fm localities, in conjunction with similar trends in hn, fe, and hg-s areas, all suggest that some dikes were emplaced after some amount of vertical-axis rotation of the lavas. Although synkinematic dike intrusion may be expected near ridge-ridge transforms, especially settings under transtension, the nearly orthogonal orientations of dikes to lava flows suggest that they were perhaps intruded prior to any tilting or rotation of lavas. If dikes were emplaced after some rotation of lavas, then caution must be used when using curved patterns of dike strikes alone as passive markers to infer simple shear, as dikes may have been intruded in nonuniform initial orientations and may be less rotated than predicted.

Statistically distinct locality mean remanence directions from most study localities across Flateyjarskagi are interpreted to indicate differential structural rotations of crustal blocks south of the HFF. The progressive clockwise deflection of remanence declinations with proximity to the fault zone mimics the clockwise curvature of mean lava flow and dike strikes (Figure 9b) and broadly supports a structural model with increasing rotation toward the fault zone. However, the clockwise deflection in remanence directions is not smoothly varying, but rather appears to change abruptly over relatively short distances. The best example is from subareas hg-s to hg-n that exhibit a distinct change in directions across the subtle Gil-Látur Line. Directions from hg-n subarea and the next area ~3 km to the north (hp) are indistinguishable, implying

that they lie within the same crustal block or in blocks that rotated similarly. However, the next localities farther north, fm and hn, yield locality mean directions that are indistinguishable from each other, yet both appear to be distinct from hg-n and hp. Distinct directions from subsidiary localities near the fault zone also suggest differential rotation between individual crustal blocks parallel to the HFF.

5.3. Rotation Estimates

The magnitude of crustal block rotation inferred from distinct locality mean directions is dependent on the method employed, and several different methods of tectonic analysis are investigated. The most structurally plausible rotational history should restore observed remanence directions and structures back to their expected initial orientations; however, unique reconstructions are challenging due to the complex history and various possible rotation sequences associated with major transforms, and lack of well-constrained geochronology. Due to the evidence that some dikes were emplaced in different orientations during deformation, we choose to not assume initial dike orientations but rather restore the lavas to horizontal orientations and the locality mean directions to a GAD expected direction.

One common approach is to first carry out a tilt-correction to restore lavas to their assumed initial horizontal orientation. This simple "backtilt" appears to restore locality mean directions from the two southernmost study localities (gr and hg-s) farthest from the HFF, and one closer (fe). However, locality mean directions from the other localities are all distinct from the GAD expected direction at the 95% confidence level, indicating that some additional rotation or component of vertical-axis rotation is required (Figures 6 and 7). The differences in tilt-corrected declinations suggest differing amounts of some component of clockwise vertical-axis rotation, or other rotations have affected the region up to about 12 km south of the fault zone (Figure 9c and Table 1). However, tilt corrections may produce considerable declination anomalies that may be incorrectly interpreted as vertical-axis rotations (MacDonald, 1980). Therefore, the tilt correction is not applicable for areas that have experienced multiple deformational events or different styles of deformation throughout their history (MacDonald, 1980). Multiple deformational events are expected in Flateyjarskagi where extensive geologic evidence supports the complex evolution of the crust from emplacement, rift-related subsidence and tilting, and subsequent development and evolution of the HFF. Because a tilt correction does not fully restore mean directions from all areas, or account for the clockwise change in dike strike, a further tectonic analysis approach is necessary.

Although an array of possible sequences of horizontal-axis and vertical-axis rotations could produce the observed locality mean directions and structural orientations, the exact sequence of deformation events is unknown. Rather than arbitrarily assign a sequence of events, we prefer to solve for a single rotation about an inclined axis that restores the data to expected directions. The sinistral oblique slip on NNE striking faults broadly supports the interpretation of a best fit inclined rotation axis. The best fit inclined rotation axis can be calculated with a rotation magnitude that restores both area mean vectors and normals to lavas to expected orientations. Uncertainties on the amounts of rotation (ΔR of Demarest, 1983) were calculated using locality mean directions and the larger uncertainty (either η_{95} or $\zeta_{,95}$), and α_{95} of 5.0° for GAD expected direction. In general, best fit inclined axes and magnitudes of rotation vary systematically with proximity to the HFF (Figure 9d and Table 1). Best fit rotation axes have predominantly SSE trends with shallower plunges for distal areas and steeper plunges for areas more proximal to the fault zone, and amounts of rotation generally increase toward the HFF. Rotations range from 23° ± 13° to 74° ± 7° across the main study areas, and 56° ± 21° to 145° ± 29° for the subsidiary areas closer to the HFF (Figure 9d and Table 1). Although based on directions from few sites, rotation amounts appear to vary across three subsidiary study areas that are located along a transect ~4.3 km south from and parallel to the fault zone. From east to west across ~10 km, rotation amounts range from 56 ± 21° (fe) to 93° ± 16° (fn) to 96° ± 9° (hn).

One final estimate on the amount of rotation is provided by a combination of all northern Flateyjarskagi data from 108 sites <12 km to the HFF zone (Figure S2 and Table 1). A bootstrapped grand mean direction of declination/inclination = 105.4°/53.7°, n = 108, η_{95} = 2.6, $\zeta_{,95}$ = 3.6, (α_{95} = 3.2°), and average lava flow orientation within each locality can be used to calculate a tilt-corrected direction and an alternative possible rotation about a best fit inclined axis. The tilt-corrected direction of dec/inc = 065.2°/80.3° implies a possible residual amount of vertical axis rotation of approximately 65° ± 7°. Implicit in this scenario is that all the vertical-axis rotation occurred before any tilting of the lavas. An alternative best fit inclined axis rotation of 55° ± 7° would restore all the northern data and average lava flow orientations to expected directions (Table 1). Since the

inclined-axis rotation makes no assumption about the sequence of events, this solution is preferred in this case where the sequence of deformation events is unknown. However, we note that both methods yield similar amounts of rotation for all the northern sites combined, demonstrating overall support for large rotations of crustal blocks in northern Flateyjarskagi.

5.4. Structural Rotation Model for Distributed Deformation Near the TFZ

Large-magnitude vertical-axis rotations of crustal blocks near continental transform fault zones have long been determined by paleomagnetic analysis (e.g., Luyendyk et al., 1980), yet only one other location, in the Troodos Ophiolite, has revealed exposures of an oceanic transform to study in detail. Field geologic relationships combined with paleomagnetic analyses of dikes in the Troodos Ophiolite documented increasing deformation and progressive rotation approaching the Arakapas Transform Fault Zone (Allerton & Vine, 1987; Bonhommet et al., 1988; MacLeod & Murton, 1993; Morris et al., 1990). Although no detailed kinematic model was proposed to explain the rotations near the Arakapas Transform until recently (Scott et al., 2013), many studies of other oceanic transform zones and the South Iceland Seismic Zone have led others toward a bookshelf faulting model (Cowan et al., 1986; Einarsson & Eiríksson, 1982; Kleinrock & Hey, 1989; Phipps Morgan & Kleinrock, 1991; Wetzel et al., 1993). A bookshelf mechanism was also recently proposed to explain strike-slip focal mechanisms for earthquakes located between overlapping volcanic systems in the Northern Volcanic Zone in Iceland, with crustal blocks about 15 km long and 2 km wide (Green et al., 2014). However, these examples may not be directly applicable to the scale and style of deformation within the TFZ in northern Iceland.

Despite the relatively simple and continuous overall structural curvature observed in the spatial patterns of the strike of lava flows, dikes, and faults across Flateyjarskagi, the paleomagnetic data show abrupt changes and a range of block rotations that help to refine the mechanisms responsible for the distributed deformation. The consistent clockwise deflection of both paleomagnetic declinations and field structures near the HFF implies a deformation mechanism that includes increasing block rotation toward the HFF Zone, effectively ruling out the transform-parallel slip model (Figure 2b). The large, variable rotations, and extensive faults, fractures, and veins in a range of orientations observed at these shallow crustal depths (1 to 1.5 km), indicate that the pervasive and continuous simple shear mechanism (Figure 2c) does not represent the best approximation for describing distributed brittle deformation near the HFF. Both the bookshelf model (Figure 2d) and small blocks with variable internal rotation model (Figure 2e) include extensive faulting across the entire shear zone, rotation of crustal blocks, and are considered more likely representations. However, a simple bookshelf model alone cannot explain the large and variable rotations of crustal blocks near the HFF. Mean remanence directions are not consistent between areas perpendicular or parallel to the HFF, indicating that a simple bookshelf model is not applicable at the scale of the entire deforming region on land ($>$100 km^2). The increase in fault density near the HFF generally supports a decrease in crustal block area with proximity to the major transform zone, and thus, blocks are much smaller ($\leq$ few kilometers across) than the width of the deformation zone ($\geq$10 km). Furthermore, small triangular-shaped basins or other extensional features are not observed at the edges (shelf of the books), although paleomagnetic and subtle structural evidence support the previous interpretation that the Gil-Látur Line is a structural boundary or discrete fault zone subparallel to the HFF and may be relatively continuous. Although the paleomagnetic data are not sufficient to directly disprove the bookshelf model may be operating at greater distances from the HFF zone, or at a smaller scale within individual crustal blocks, the data more strongly support the small block model with variable rotations in the immediate vicinity of the HFF.

A plausible scenario for the tectonic history of northern Flateyjarskagi includes the following generalized sequence that began with the formation of the HFF ~7 Ma. Strong coupling along the developing fault zone resulted in distributed deformation that may have accommodated initial shearing on reactivated rift-parallel normal faults in a bookshelf-like model. As shearing continued, and rotation of crustal blocks and their bounding faults approached the theoretical rotation limit (~20° to 45°) permitted by one set of faults (Nur et al., 1986), a new set of faults formed to accommodate additional shearing. The formation of a new array of faults would effectively subdivide crustal blocks further, in essence modifying the bookshelf mechanism with additional generations of faults. This process would result in relatively small blocks that could rotate independently, and perhaps more than surrounding blocks (Figure 10). Because minimum and best fit rotations determined from paleomagnetic analyses in northern Flateyjarskagi may exceed the theoretical ~40° to

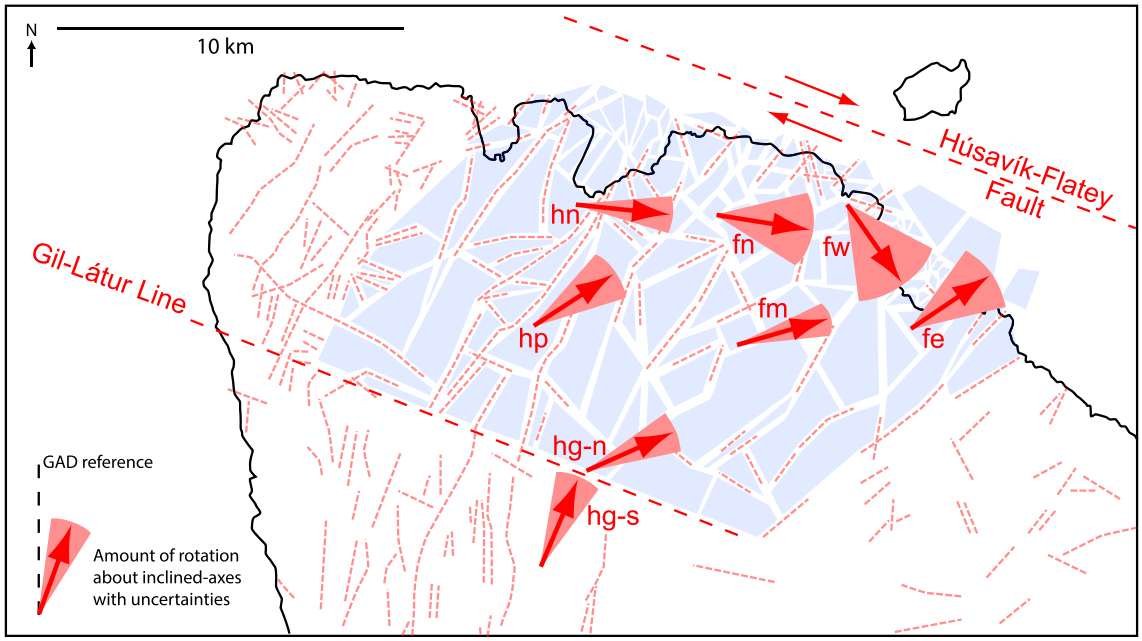

Figure 10. Schematic map of northern Flateyarskagi highlights the spatial variation in the amounts of rotation (red arrows) about best fit inclined axes with associated uncertainties. Differential amounts of rotation in study areas both perpendicular and parallel to the HFF are consistent with small block model with variable rotation. Possible crustal block geometries (shaded areas) are inferred from spatial distribution of faults (dashed red lines) after Young et al. (1985).

45° limit, more than one (or two) generation(s) of faults must accommodate the large rotations adjacent to the HFF Zone. We cannot exclude an alternative possibility that during initial formation of the HFF zone, sets of faults (e.g., Riedel shears) or other associated shear fractures could have developed that would have also subdivided the crustal blocks into smaller irregular shapes without a prior bookshelf-type sequence. Although no systematic cross-cutting relationships were observed, numerous faults with a range of orientations are present across northern Flateyjarskagi, and extrapolation of previously mapped faults across the study area yields irregularly shaped crustal blocks (Figure 10). Although more detailed mapping of the spatial distributions of faults with specific kinematic data might document the dimensions and exact nature of crustal block boundaries, discontinuous and covered exposures may preclude distinguishing any unique block geometries or structural evolution.

5.5. Implications for Oceanic Transform Deformation

The transform deformation in oceanic-like crust of north Iceland supports a modified bookshelf mechanism with small crustal blocks that experience variable amounts of rotation adjacent to a major transform boundary. In comparison to other oceanic transforms, the Tjörnes Fracture Zone may be somewhat different due to its proximity to the Iceland hot spot, affecting the thermal structure and producing thicker than average crust, as well as transform migration associated with the northward propagating Northern Volcanic Zone. Nonetheless, the deformation in the upper crust of northern Iceland near the main HFF is considered to be similar to other oceanic crust as the behavior is likely controlled by mechanical anisotropy (faults, fractures, and dikes) formed at ridges and rifts. As shearing progresses, reactivated slip along preexisting zones of weakness may be more favorable than creation of a new fault (Nur et al., 1986; Phipps Morgan & Kleinrock, 1991), or a new array of subparallel faults may form (Einarsson, 1991). Although a bookshelf faulting mechanism is commonly thought to operate within propagating rift systems in oceanic crust, it may also be associated with anti-J-shaped abyssal hill curvatures observed near other transform faults, and perhaps within the tectonized zone of some other oceanic transforms.

Although the bookshelf model may account for the formation of curved, anti-J-shaped lineaments documented near oceanic transforms, deformation closer to the transform is notably more challenging to quantify. Lineament-bounded blocks with consistent orientations with respect to the Sovanco Fracture Zone along the Juan de Fuca Ridge are hypothesized to have rotated about 30° (Cowan et al., 1986). Anti-J-shaped

lineations near the Clipperton transform along the East Pacific Rise deviate from ridge parallel by as much as 15° to 20°, although the abyssal hills are difficult to locate within 8 to 10 km of the transform due to later deformation (Sonder & Pockalny, 1999). Maximum anti-J-shaped deflections relative to regional abyssal hill trends at Pacific-Antarctic ridge-transform intersections vary between 22° and 63° (Croon et al., 2010). Increased distributed deformation associated with the formation of anti-J-shaped bathymetric lineations can be correlated with times of increased coupling across the transform related to changes in relative plate motion (Croon et al., 2010). However, other factors could also increase coupling along a transform, such as increased friction, strain localization, or transform migration. As some seafloor lineaments approach the theoretical rotation limit permitted by one set of bookshelf faults, it seems likely that larger magnitude rotations are only possible immediately adjacent to the transform by breaking the bookshelf model. We speculate that as deformation continues, new faults will form to accommodate larger block rotations and oceanic transform systems may evolve in a similar way to that exemplified by the HFF zone in north Iceland. Because lineaments and detailed structure are poorly known within 10 km of transforms and in the tectonized zone immediately adjacent to the transform, the setting in northern Iceland offers a rare glimpse into the deformation immediately adjacent to a main oceanic transform fault. The complex deformation and large crustal block rotations proximal to the HFF provide insight into the processes underlying complicated lineament patterns that are ordinarily covered by debris and lava flows, masking more complex submarine geology near modern oceanic transforms.

6. Conclusions

Structural and paleomagnetic observations from Mid-Late Miocene basalt lavas and dikes exposed near the HFF in north Iceland indicate significant postemplacement tectonic rotations of individual crustal blocks. Paleomagnetic data support a structural model with a progressive clockwise increase in amount of rotation toward the HFF and variable amounts of rotation of crustal blocks parallel to the fault zone. Best fit models using inclined rotation axes to restore area mean remanence directions suggest large clockwise rotations (66° ± 13° to 74° ± 11°) of crustal blocks between 6 to 12 km south of the HFF, and larger clockwise rotations (96° ± 13° to 145° ± 27°) within 6 km. When considered together, all data from 108 sites within 12 km to the HFF yield a best fit inclined axis rotation of 55° ± 7°. The large amounts of rotation near the transform are consistent with a small block model in which kilometer-scale crustal blocks are variably rotated with moderate amounts of internal deformation to accommodate increased shearing proximal to the transform zone. These results imply that the numerous studies interpreting paleostress directions from structures near in the Tjörnes Fracture Zone must be reevaluated to consider crustal block rotations. More broadly, results of this study may apply to transform zones in modern oceanic crust and ophiolites.

Acknowledgments

We gratefully acknowledge Kristján Sæmundsson and Bryndís Brandsdóttir for their hospitality and assistance with field logistics, without which this work would not be possible. Work was partially supported by NSF grant OCE-0701422 (Karson). Special thanks to John J. Prucha Field Research Grants, ExxonMobil Global Geoscience Student Grant, and K. Douglas Nelson Award for additional financial assistance that helped make this study possible as part of Horst's dissertation. A very special thanks to Jeff Gee for generously accommodating Horst in the paleomagnetics lab at Scripps Institution of Oceanography, and especially for sharing many comments and exceptional suggestions for improvements on earlier drafts. Páll Einarsson, one anonymous reviewer, and Associate Editor (Augusto Rapalini) provided helpful comments that improved the text. Detailed comments from Chief Editor (John Geissman) are also appreciated, and improved the text. Thanks also to Lisa Tauxe for development of PmagPy software used to generate stereonet plots in this paper. Supporting data are included as one table in the supporting information; any additional data may be obtained from Horst (e-mail: ahorst@oberlin.edu).

References

Allerton, S., & Vine, F. J. (1987). Spreading evolution of the Troodos Ophiolite, Cyprus: Some paleomagnetic constraints. *Geology*, *19*, 637–640.

Benediktsdóttir, Á., Hey, R., Martinez, F., & Höskuldsson, Á. (2012). Detailed tectonic evolution of the Reykjanes Ridge during the past 15 Ma. *Geochemistry, Geophysics, Geosystems*, *13*, Q02008. https://doi.org/10.1029/2011GC003948

Bergerat, F., Angelier, J., & Homberg, C. (2000). Tectonic analysis of the Husavik-Flatey Fault (northern Iceland) and mechanisms of an oceanic transform zone, the Tjörnes Fracture Zone. *Tectonics*, *19*(6), 1161–1177. https://doi.org/10.1029/2000TC900022

Bergerat, F., Angelier, J., & Villemin, T. (1990). Fault systems and stress patterns on emerged oceanic ridges: A case study in Iceland. *Tectonophysics*, *179*, 1397–1403.

Besse, J., & Courtillot, V. (2002). Apparent and true polar wander and the geometry of the geomagnetic field over the last 200 Myr. *Journal of Geophysical Research*, *107*(B11), 2300. https://doi.org/10.1029/2000JB000050

Bonhommet, N., Roperch, P., & Calza, F. (1988). Palaeomagnetic arguments for block rotations along the Arakapas fault (Cyprus). *Geology*, *16*(5), 422–425. https://doi.org/10.1130/0091-7613(1988)016%3C0422:PAFBRA%3E2.3.CO;2

Brandsdóttir, B., Einarsson, P., Detrick, R. S., Mayer, L., Calder, B., Driscoll, N., & Richter, B. (2003). Lost in Iceland? Fracture zone complications along the Mid-Atlantic Plate Boundary. *Eos, Transactions American Geophysical Union*, *84*(46). fall meet. Suppl., Abstract T22A-0504

Cowan, D. S., Botros, M., & Johnson, H. P. (1986). Bookshelf tectonics: Rotated crustal blocks within the sovanco fracture zone. *Geophysical Research Letters*, *13*(10), 995–998. https://doi.org/10.1029/GL013i010p00995

Crane, K. (1976). The intersection of the Siqueiros Transform Fault and the East Pacific Rise. *Marine Geology*, *21*(1), 25–46. https://doi.org/10.1016/0025-3227(76)90102-X

Croon, M. B., Cande, S. C., & Stock, J. M. (2010). Abyssal hill deflections at Pacific-Antarctic ridge-transform intersections. *Geochemistry, Geophysics, Geosystems*, *11*, Q1104. https://doi.org/10.1029/2010GC003236

Demarest, H. H. (1983). Error analysis for the determination of tectonic rotation from paleomagnetic data. *Journal of Geophysical Research*, *88*(B5), 4321–4328. https://doi.org/10.1029/JB088iB05p04321

DeMets, C., Gordon, R. G., & Argus, D. F. (2010). Geologically current plate motions. *Geophysical Journal International*, *181*(1), 1–80. https://doi.org/10.1111/j.1365-246X.2009.04491.x

Einarsson, P. (1976). Relative locations of earthquakes within the Tjörnes Fracture Zone. *Soc. Sci. Islandica*, Greinar V, 45–60.

Einarsson, P. (1987). Compilation of earthquake fault plane solutions in the North Atlantic. In K. Kashahara (Ed.), *Recent Plate Movements and Deformation* (pp. 47–62). Washington, DC: American Geophysical Union.
Einarsson, P. (1991). Earthquakes and present-day tectonism in Iceland. *Tectonophysics*, *189*(1-4), 261–279. https://doi.org/10.1016/0040-1951(91)90501-I
Einarsson, P. (2008). Plate boundaries, rifts and transforms in Iceland. *Jökull*, *58*, 35–58.
Einarsson, P., & Eiríksson, J. (1982). Earthquake fractures in the districts land and Rangarvellir in the South Iceland Seismic Zone. *Jökull*, *32*, 113–119.
Fisher, R. (1953). Dispersion on a sphere. *Proceedings of the Royal Society of London*, *217*(1130), 295–305. https://doi.org/10.1098/rspa.1953.0064
Fjäder, K., Gudmundsson, A., & Forslund, T. (1994). Dikes, minor faults and mineral veins associated with a transform fault in north Iceland. *Journal of Structural Geology*, *16*(1), 109–119. https://doi.org/10.1016/0191-8141(94)90022-1
Fornari, D. J., Gallo, D. G., Edwards, M. H., Madsen, J. A., Perfit, M. R., & Shor, A. N. (1989). Structure and topography of the Siqueiros transform fault system: Evidence for the development of intra-transform spreading centers. *Marine Geophysical Researches*, *11*(4), 263–299. https://doi.org/10.1007/BF00282579
Fox, P. J., & Gallo, D. G. (1984). A tectonic model for ridge-transform-ridge plate boundaries: Implications for the structure of oceanic lithosphere. *Tectonophysics*, *104*(3-4), 205–242. https://doi.org/10.1016/0040-1951(84)90124-0
Francheteau, J., Choukroune, P., Hekinian, R., LePichon, X., & Needham, H. D. (1976). Oceanic fracture zones do not provide deep sections in the crust. *Canadian Journal of Earth Sciences*, *13*(9), 1223–1235. https://doi.org/10.1139/e76-124
Freund, R. (1974). Kinematics of transform and transcurrent faults. *Tectonophysics*, *21*(1-2), 93–134. https://doi.org/10.1016/0040-1951(74)90064-X
Garcia, S., Angelier, J., Bergerat, F., & Homberg, C. (2002). Tectonic analysis of an oceanic transform fault zone based on fault-slip data and earthquake focal mechanisms; the Husavik-Flatey fault zone, Iceland. *Tectonophysics*, *344*(3–4), 157–174. https://doi.org/10.1016/S0040-1951(01)00282-7
Green, R. G., White, R. S., & Greenfield, T. (2014). Motion in the north Iceland volcanic rift zone accommodated by bookshelf faulting. *Nature Geoscience*, *7*(1), 29–33. https://doi.org/10.1038/ngeo2012
Grindlay, N. R., & Fox, P. J. (1993). Lithospheric stresses associated with nontransform offsets of the Mid-Atlantic ridge: Implications from a finite element analysis. *Tectonics*, *12*(4), 982–1003. https://doi.org/10.1029/93TC00364
Grindlay, N. R., Fox, P. J., & Macdonald, K. C. (1991). Second-order ridge axis discontinuities in the south Atlantic: Morphology, structure, and evolution. *Marine Geophysical Researches*, *13*(1), 21–49. https://doi.org/10.1007/BF02428194
Gudmundsson, A., & Fjäder, K. (1995). Dikes, minor faults and mineral veins associated with a transform fault in North Iceland: Reply. *Journal of Structural Geology*, *17*(11), 1633–1636. https://doi.org/10.1016/0191-8141(95)00072-L
Hardarson, B. S., Fitton, J. G., Ellam, R. M., & Pringle, M. S. (1997). Rift relocation - a geochemical and geochronological investigation of a palaeo-rift in northwest Iceland. *Earth and Planetary Science Letters*, *153*(3-4), 181–196. https://doi.org/10.1016/S0012-821X(97)00145-3
Hey, R., Martinez, F., Höskuldsson, Á., & Benediktsdóttir, Á. (2010). Propagating rift model for the V-shaped ridges south of Iceland. *Geochemistry, Geophysics, Geosystems*, *11*, Q03011. https://doi.org/10.1029/2009GC002865
Hey, R. N., Duennebier, F. K., & Morgan, W. J. (1980). Propagating rifts on mid-ocean ridges. *Journal of Geophysical Research*, *85*(B7), 3647–3658. https://doi.org/10.1029/JB085iB07p03647
Homberg, C., Bergerat, F., Angelier, J., & Garcia, S. (2010). Fault interaction and stresses along broad oceanic transform zone: Tjörnes Fracture Zone, north Iceland. *Tectonics*, *29*, TC1002. https://doi.org/10.1029/2008TC002415
Jancin, M., Young, K. D., Voight, B., Aronson, J. L., & Sæmundsson, K. (1985). Stratigraphy and K/Ar ages across the west flank of the northeast Icelandic axial rift zone, in relation to the 7 Ma volcano-tectonic reorganization of Iceland. *Journal of Geophysical Research*, *90*(B12), 9961–9985. https://doi.org/10.1029/JB090iB12p09961
Jancin, M., Young, K. D., Voight, B., & Orkan, N. I. (1995). Dikes, minor faults and mineral veins associated with a transform fault in north Iceland: Discussion. *Journal of Structural Geology*, *17*(11), 1627–1631. https://doi.org/10.1016/0191-8141(95)00073-M
Karson, J. A. (1986). Lithosphere age, depth and structural complications resulting from migrating transform faults. *Journal of the Geological Society of London*, *143*(5), 785–788. https://doi.org/10.1144/gsjgs.143.5.0785
Kastens, K. A., Ryan, W. B. F., & Fox, P. J. (1986). Structural and volcanic expression of a fast slipping ridge-transform-ridge boundary: Sea MARC I and photographic surveys at the Clipperton Transform Fault. *Journal of Geophysical Research*, *91*(B3), 3469–3488. https://doi.org/10.1029/JB091iB03p03469
Kirschvink, J. L. (1980). The least-squares line and plane and the analysis of palaeomagnetic data. *Geophysical Journal of the Royal Astronomical Society*, *62*(3), 699–718. https://doi.org/10.1111/j.1365-246X.1980.tb02601.x
Kleinrock, M. C., & Hey, R. N. (1989). Migrating transform zone and lithospheric transfer at the Galapagos 95.5°W propagator. *Journal of Geophysical Research*, *94*(B10), 13,859–13,878. https://doi.org/10.1029/JB094iB10p13859
Kristjánsson, L. (2009). A new study of paleomagnetic directions in the Miocene lava pile between Arnarfjörður and Breiðaförður in the Vestfirðir peninsula, Northwest Iceland. *Jökull*, *59*, 33–50.
LaFemina, P. C., Dixon, T. H., Malservisi, R., Amadottis, T., Sturkell, E., Sigmundsson, F., & Einarsson, P. (2005). Geodetic GPS measurements in south Iceland: Strain accumulation and partitioning in a propagating ridge system. *Journal of Geophysical Research*, *110*, B11405. https://doi.org/10.1029/2005JB003675
Långbacka, B. O., & Gudmundsson, A. (1995). Extensional tectonics in the vacinity of a transform fault in north Iceland. *Tectonics*, *14*(2), 294–306. https://doi.org/10.1029/94TC02904
Lonsdale, P. (1977). Structural geomorphology of a fast-spreading rise crest: The East Pacific Rise crest at 3°25'S. *Marine Geophysical Researches*, *3*(3), 251–293. https://doi.org/10.1007/BF00285656
Luyendyk, B. P., Kamerling, M. J., & Terres, R. (1980). Geometrical model for Neogene crustal rotations in southern California. *Geological Society of America Bulletin*, *91*(4), 211–217. https://doi.org/10.1130/0016-7606(1980)91%3C211:GMFNCR%3E2.0.CO;2
Macdonald, K. C., Fox, P. J., Alexander, R. T., Pockalny, R., & Gente, P. (1996). Volcanic growth faults and the origin of Pacific abyssal hills. *Nature*, *380*(6570), 125–129. https://doi.org/10.1038/380125a0
MacDonald, W. D. (1980). Net tectonic rotation, apparent tectonic rotation, and the structural tilt correction in paleomagnetic studies. *Journal of Geophysical Research*, *85*(B7), 3659–3669. https://doi.org/10.1029/JB085iB07p03659
MacLeod, C. J., & Murton, B. J. (1993). Structure and tectonic evolution of the southern Troodos transform fault zone, Cyprus. In A. Prichard, T. Alabaster, N. Harris, & C. Neary (Eds.), *Magmatic processes and plate tectonics*, *special publication* (Vol. 76, pp. 141–176). London: Geological Society of London.

Magnúsdóttir, S., Brandsdóttir, B., Driscoll, N., & Detrick, R. (2015). Postglacial tectonic activity within the Skjálfandjúp Basin, Tjörnes Fracture Zone, offshore Northern Iceland, based on high resolution sesimic stratigraphy. *Marine Geology*, *367*, 159–170. https://doi.org/10.1016/j.margeo.2015.06.004

Mandl, G. (1987). Tectonic deformation by rotating parallel faults—The 'bookshelf' mechanism. *Tectonophysics*, *141*(4), 277–316. https://doi.org/10.1016/0040-1951(87)90205-8

McDougall, I., Kristjánsson, L., & Sæmundsson, K. (1984). Magnetostratigraphy and geochronology of Northwest Iceland. *Journal of Geophysical Research*, *89*, 3659–3669.

McKenzie, D. (1986). The geometry of propagating rifts. *Earth and Planetary Science Letters*, *77*(2), 176–186. https://doi.org/10.1016/0012-821X(86)90159-7

McKenzie, D., & Jackson, J. (1983). The relationship between strain rates, crustal thinning, paleomagnetism, finite strain, and fault movements within a deforming zone. *Earth and Planetary Science Letters*, *65*(1), 182–202. https://doi.org/10.1016/0012-821X(83)90198-X

McMaster, R. L., Schilling, J. E., & Pinet, P. R. (1977). Plate boundary within Tjörnes Fracture Zone on northern Iceland's insular margin. *Nature*, *269*(5630), 663–668. https://doi.org/10.1038/269663a0

Metzger, S., & Jónsson, S. (2014). Plate boundary deformation in North Iceland during 1992–2009 revealed by InSAR time-series analysis and GPS. *Tectonophysics*, *634*, 127–138. https://doi.org/10.1016/j.tecto.2014.07.027

Morris, A., Creer, K. M., & Robertson, A. H. F. (1990). Paleomagnetic evidence for clockwise rotations related to dextral shear along the Southern Troodos Transform Fault, Cyprus. *Earth and Planetary Science Letters*, *99*(3), 250–262. https://doi.org/10.1016/0012-821X(90)90114-D

Nelson, M. R., & Jones, C. H. (1987). Paleomagnetism and crustal rotations along a shear zone, Las Vegas Range, southern Nevada. *Tectonics*, *6*(1), 13–33. https://doi.org/10.1029/TC006i001p00013

Nur, A., Ron, H., & Scotti, O. (1986). Fault mechanics and the kinematics of block rotations. *Geology*, *14*(9), 746–749. https://doi.org/10.1130/0091-7613(1986)14%3C746:FMATKO%3E2.0.CO;2

OTTER Team (1985). The geology of the oceanographer transform: The transform domain. *Marine Geophysical Researches*, *7*, 329–358.

Pálmason, G., & Sæmundsson, K. (1974). Iceland in relation to the Mid-Atlantic Ridge. *Annual Review of Earth and Planetary Sciences*, *2*(1), 25–50. https://doi.org/10.1146/annurev.ea.02.050174.000325

Phipps Morgan, J., & Kleinrock, M. C. (1991). Transform zone migration: Implications of bookshelf faulting at oceanic and Icelandic propagating ridges. *Tectonics*, *10*(5), 920–935. https://doi.org/10.1029/90TC02481

Rögnvaldsson, S. T., Gudmundsson, A., & Slunga, R. (1998). Seismotectonic analysis of the Tjörnes Fracture Zone, an active transform fault in north Iceland. *Journal of Geophysical Research*, *103*(B12), 30,117–30,129. https://doi.org/10.1029/98JB02789

Sæmundsson, K. (1974). Evolution of the axial rifting zone in northern Iceland and the Tjornes Fracture Zone. *Geological Society of America Bulletin*, *85*(4), 495–504. https://doi.org/10.1130/0016-7606(1974)85%3C495:EOTARZ%3E2.0.CO;2

Sæmundsson, K. (1979). Outline of geology of Iceland. *Jökull*, *29*, 7–28.

Scott, C. P., Titus, S. J., & Davis, J. R. (2013). Using field data to constrain a numerical kinematic model for ridge-transform deformation in the Troodos ophiolite, Cyprus. *Lithosphere*, *5*, 109–127. https://doi.org/10.1130/L237.1

Searle, R. C. (1986). GLORIA investigations of oceanic fracture zones: Comparative study of the transform fault zone. *Journal of Geology Society of London*, *143*(5), 743–756. https://doi.org/10.1144/gsjgs.143.5.0743

Sigmundsson, F., Einarsson, P., Bilham, R., & Sturkell, E. (1995). Rift-transform kinematics in south Iceland: Deformation from Global Positioning System measurements, 1986 to 1992. *Journal of Geophysical Research*, *100*(B4), 6235–6248. https://doi.org/10.1029/95JB00155

Sonder, L. J., & Pockalny, R. A. (1999). Anomalously rotated abyssal hills along active transforms: Distributed deformation of oceanic lithosphere. *Geology*, *27*(11), 1003–1006. https://doi.org/10.1130/0091-7613(1999)027%3C1003:ARAHAA%3E2.3.CO;2

Stefansson, R., Gudmundsson, G. B., & Halldorsson, P. (2008). Tjörnes fracture zone. New and old seismic evidences for the link between North Iceland rift zone and the Mid-Atlantic ridge. *Tectonophysics*, *447*(1-4), 117–126. https://doi.org/10.1016/j.tecto.2006.09.019

Tapponnier, P., Armijo, R., Manighetti, I., & Courtillot, V. (1990). Bookshelf faulting and horizontal block rotations between overlapping rifts in southern Afar. *Geophysical Research Letters*, *17*(1), 1–4. https://doi.org/10.1029/GL017i001p00001

Tauxe, L. (2010). *Essentials of paleomagnetism* (p. 512). Berkeley: University of California Press.

Tauxe, L., Kylstra, N., & Constable, C. (1991). Bootstrap statistics for paleomagnetic data. *Journal of Geophysical Research*, *96*(B7), 11,723–11,740. https://doi.org/10.1029/91JB00572

Tucholke, B. E., & Schouten, H. (1988). Kane fracture zone. *Marine Geophysical Researches*, *10*(1-2), 1–39. https://doi.org/10.1007/BF02424659

Ward, P. L. (1971). New interpretation of the geology of Iceland. *Geological Society of America Bulletin*, *82*(11), 2991–3012. https://doi.org/10.1130/0016-7606(1971)82%5B2991:NIOTGO%5D2.0.CO;2

Wetzel, L. R., Wiens, D. A., & Kleinrock, M. C. (1993). Evidence from earthquakes for bookshelf faulting at large non-transform ridge offsets. *Nature*, *362*(6417), 235–237. https://doi.org/10.1038/362235a0

Young, K. D., Jancin, M., Voight, B., & Orkan, N. I. (1985). Transform deformation of tertiary rocks along the Tjörnes Fracture Zone, north central Iceland. *Journal of Geophysical Research*, *90*(B12), 9986–10,010. https://doi.org/10.1029/JB090iB12p09986